



Universiteit Utrecht

Speciation of Sulfur in Peat in Four Locations in the Northwestern Netherlands

Following the American Psychological Association's Guidelines

Jiwon Kim

Student Number: 4299361

Course Code: UCSCIRES32

University College Utrecht

Supervisor: Jasper Griffioen

August 2017

Word Count: 6922

Abstract

The peat areas in the Netherlands demonstrate a high amount of sulfur of up to 8-9 wt%. In order to investigate the S speciation in Dutch peat, peat samples from four locations in the northwestern Netherlands were analyzed. The three main objectives of this study are: to determine the relative abundance of elemental S in comparison to the other inorganic S species; to examine whether the availability of reactive iron is associated with the presence of elemental sulfur in peat; and to search for, if any, differences in S speciation between peat from a marine and that from a fluvial paleoenvironment. Sequential wet chemical extraction of S was performed to fractionate the total S into different inorganic sulfur species, such as acid volatile sulfur (AVS), elemental sulfur, and chromium-reducible sulfur (CRS). In all samples, pyritic S was the dominant inorganic S species, followed by AVS, SO_4^{2-} , and S^0 . The concentrations of S^0 were consistently low in all samples, revealing no significant correlation with reactive Fe availability. The S content in marine and fluvial paleoenvironment differed with respect to the balance between total inorganic and organic S fraction, where the riverine peat demonstrated a higher total S and total inorganic S fraction than the marine peat. Future researchers of Dutch peat may benefit from these findings, as they reveal the relative abundance of different inorganic S species with the addition of elemental S to the inorganic S species.

Introduction

Understanding the mechanism of sulfur cycling in peat is crucial in the study of sulfur speciation in peat. Sulfur usually enters a wetland through groundwater and terrestrial runoff as sulfate, which is then assimilated into the sediment by plants as carbon-bound sulfur (Bates, Spiker & Holmes, 1998). Sulfate can also be reduced to hydrogen sulfide (H_2S) by sulfate reducing bacteria, which is known as dissimilatory sulfate reduction. The amount of H_2S produced depends on the availability of organic matter and the amount of sulfate present, as the sulfate reducing bacteria use organic matter as a substrate (Price & Casagrande, 1991). H_2S binds with available reactive Fe in the sediment to form iron sulfides (FeS and FeS_2). When there is a lack of available reactive Fe, porewater H_2S can react with organic matter to form organosulfur compounds; be diffused upwards to the surface where it becomes oxidized to sulfate; or be oxidized by sulfur oxidizing bacteria to sulfate or other sulfur species, such as elemental sulfur, polysulfides, and thiosulfate (Bates et al., 1998).

An existing body of research has extensively discussed the origins of sulfur in peat, revealing that there are internal processes other than the abovementioned external S sources that are changing S speciation and influencing sulfate concentrations in peat. Many have argued that oxidation of peat and pyrite is the most important internal source of sulfate (Lamers, Tomassen & Roelofs, 1998; Vermaat et al., 2016).

While mineralization of peat occurs via microbial processes, such as the abovementioned dissimilatory sulfate reduction, recent anthropogenic activities have largely contributed to the mineralization of peat and pyrite. The Netherlands has implemented a water distribution scheme, which allows inlet water from River Rhine to artificially maintain a surface water level in polders during the summer and to prevent desiccation. This measure has brought about an

increased mobilization of S in peat in the Netherlands through a number of ways. First, the concentration of sulfate in the River Rhine has been anthropogenically increased and now measures twice the concentration measured in 1900 (Smolders, Lamers, Lucassen, Velde & Roelofs, 2006). Second, the Rhine water is alkaline. Roelofs (1991) reported that the supply of alkaline water that is enriched with sulfate and bicarbonate increased reduction processes in the soil. This further led to internal eutrophication, resulting in increased levels of reduced compounds, such as sulfides. Consequently, the high input of sulfate via inlet Rhine water, coupled with the alkalinity of the water, is responsible for the increased mineralization of peat.

Another example of the anthropogenic influence is the excessive input of fertilizers and animal manures onto the agricultural lands. The concentration of nitrate in groundwater is relatively low (4-9 mg/L) in its natural state. However, the leaching introduced by agricultural activities pollutes the shallow groundwater with nitrate, creating the condition that enables more intensive oxidation of FeS_x in association with nitrate reduction. This was evidenced by how a peat layer with pyrite was found to “coincide with the disappearance of infiltrating NO_3^- and an increase in sulfate concentrations in the ground water” (Smolders et al., 2006, p. 97). Hence, the increased nitrate leaching brings about an increase in sulfate concentrations in groundwater.

Some researchers have argued that the atmospheric S deposition is the major source of sulfur in Dutch peat (Feijtel et al., 1989; Lamers et al., 1998; Smolders et al., 2006). Watanabe et al. (2013) argued that the increased air pollution from Eurasia has contributed to the increased S concentration by emitting higher amount of gaseous ammonium sulfate aerosols. Enhanced atmospheric deposition of ammonium – together with sulfate – increases the nitrate concentration in groundwater following nitrification of ammonium in the soil. Likewise, Feijtel et al. (1989) found that atmospheric sulfur deposition and oxidation of iron sulfide in the

sediment are together the major sources of sulfate in the pore water. However, the atmospheric S deposition in the Netherlands has decreased by approximately 70% in the 1980s as a result of international legislation measures intended to reduce air pollution (Boxman, Peters & Roelofs, 2008; Marnette, Houweling, Dam & Erisman, 1993). This significant reduction in atmospheric S deposition shows that the significance of atmospheric S deposition as a major source of sulfur in Dutch peat is questionable.

The increased S concentration in Dutch peat can also be explained by drainage of peatland. The peat polders with their intensive surface water network were often used for agricultural purposes. In order to create suitable conditions for agricultural land use, the peat polders were continuously and extensively drained. This practice of continuous drainage encouraged oxidation of peat, leading to an accelerated rate of land subsidence of 2-10 mm y⁻¹ (Vermaat et al., 2016). As the top soil layer is aerated, its organic components get oxidized. Land subsides and surface water levels must be artificially lowered, exposing deeper layers of peat to oxidation. Hoogland, van den Akker & Brus (2012) studied the subsidence rate observed in the last half century and compared the rate at locations with and without peat. They found that the former showed subsidence rate up to 8 mm year⁻¹ while the latter showed only 0.7 mm year⁻¹. In line with this study, Nieuwenhuis & Schokking (1997) found that land subsidence of peaty areas in the north of Netherlands is mainly due to peat oxidation associated with the local regulation of the surface water level.

In summary, sulfur in Dutch peat originates nowadays from the internal sources and external sources such as the peat itself, inlet Rhine water, drainage of farmland, and atmospheric S deposition. However, the findings from TNO Geological Survey show that the peat areas in the Netherlands show unexpectedly high amounts of sulfur up to 8-9 %-wt (Klein et al., 2015). The

excessive amount of sulfur present relative to the amount of iron present in peat is not in line with the stoichiometric relationship between Fe and S in pyrite and C and S in organic matter, which is 1 to 2 and 100 to 1 respectively. This implies that high amounts of S are present in a yet unidentified solid phase.

The purpose of this study is to dismantle this problem and further investigate the speciation of sulfur in Dutch peat. Three subsidiary questions were formulated to focus the overall investigation: 1) What is the relative abundance of elemental S compared to the other inorganic S species? 2) Is elemental S present in peat when there is too little reactive Fe to bind all inorganic S as pyrite? 3) What are, if any, the differences in S content between peat from a marine paleoenvironment and that from a fluvial paleoenvironment in terms of the form and quantity of S? Sediment cores are collected from 4 different study sites using the analytical method of wet chemical extraction and quantification of sulfur. The total sulfur pool (“total S”) is fractionated into different inorganic sulfur species, such as acid volatile sulfur, elemental sulfur, and chromium-reducible sulfur in addition to organic-bound S.

It is expected that the S content measured in cores A and B will be relatively higher than in cores C and D due to the marine influence. The following section discusses the locations and the geographical settings of the study areas to better understand the paleoenvironmental history of the areas and its influence on the speciation of S in peat.

Study Area

Four sediment cores were collected from four different locations (Figure 1). Sites A and B are located to the north of Amsterdam (‘Holland’) near boreholes B19H0864 and B25E1030, respectively. Sites C and D are located in the riverine area southwest to Utrecht near boreholes B38E0306 and B38G2112, respectively. The depth of sampling for each site was determined

prior to fieldwork by studying the sediment composition characteristics of the already existing boreholes. Figure 2 shows depth profiles of these boreholes, including the geological units, lithoclass, and the sediment lithology. These specific locations were chosen because peat with high S contents was found at these previously studied boreholes, specifically Holland Peat from the Nieuwkoop Formation (coded as NIHO).

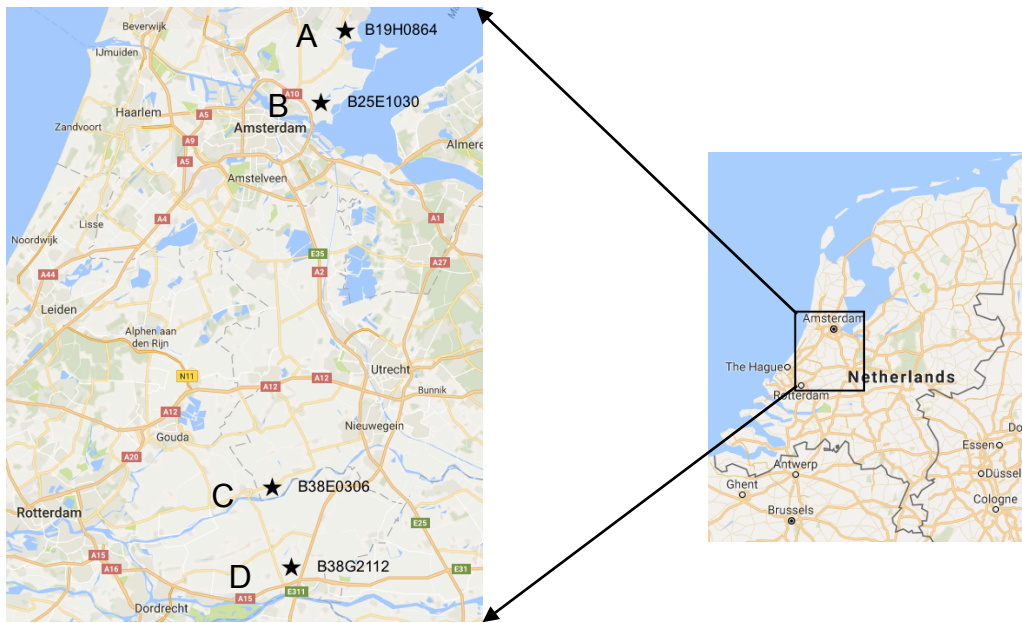


Figure 1. Map of the study area with the locations of the sampling sites.

The peat layers at the study sites belong to the upper peat layer of the stratigraphic unit Holland Peat ('Hollandveen Laagpakket') of the Nieuwkoop Formation, formed during the Subboreal period (Figure 3). This belongs to the Holocene epoch, which started at 11 700 BP and is characterized by a warmer climate after the last glacial period (Yu et al., 2009). The Holland Peat covers most peat surface in the provinces of North Holland, Utrecht, and South Holland, consisting of eutrophic peat (wood peat) in the base layer and oligotrophic peat (*Sphagnum* peat)

towards the top (Zagwijn, 1986). The thickness ranges from 0.1 m to 5 m (Erkens, van der Meulen & Middelkoop, 2016), which is also evident in Figure 2.

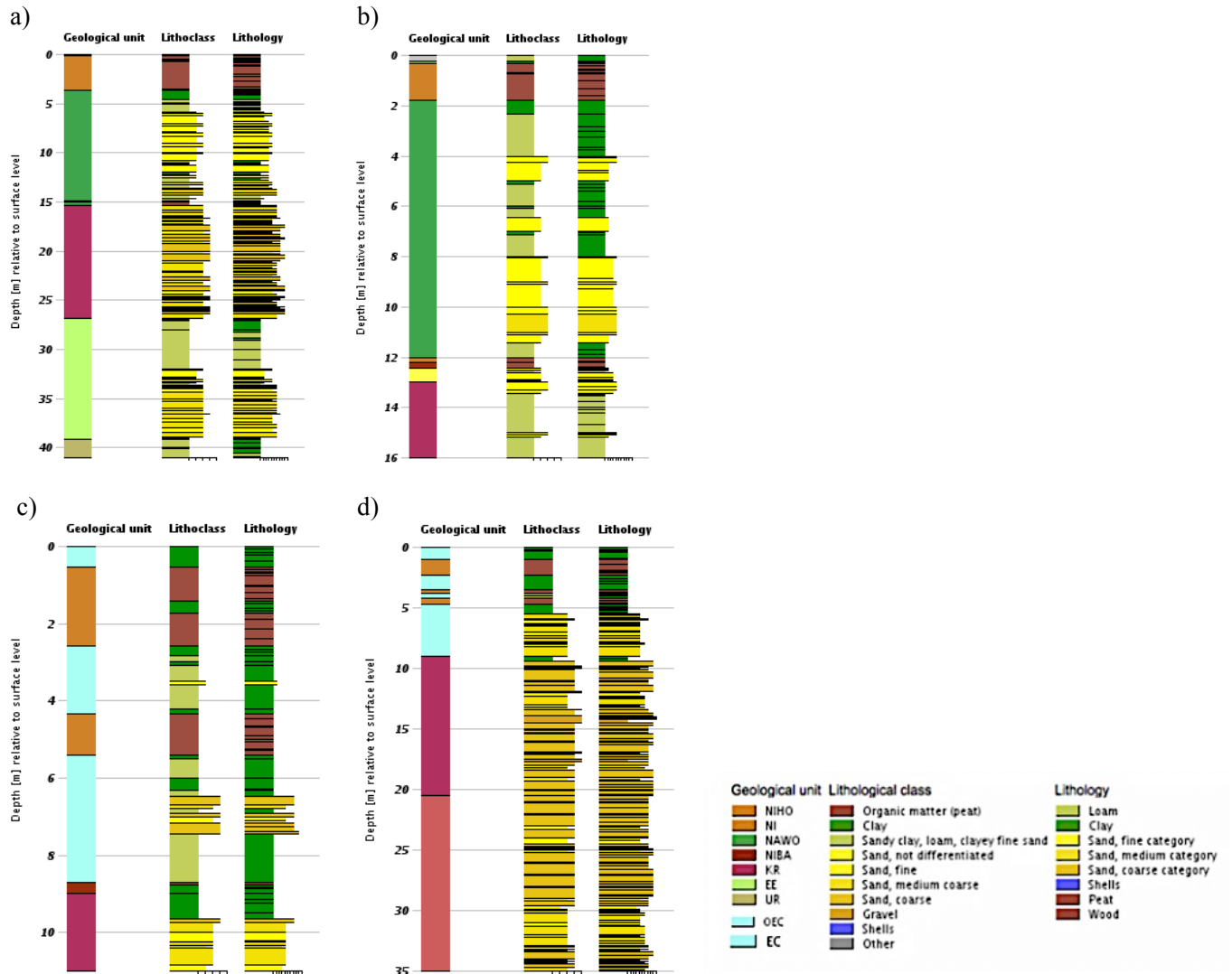


Figure 2. Borehole descriptions including the geological unit, lithoclass, and lithology: a) borehole B19H0864; b) B25E1030; c) B38E0306; d) B38G2112. Taken from DINO-database of Holland area and Utrecht River Area, Netherlands.

It is important to note the marked contrast between the paleoenvironmental history of the study areas. Sites A and B located in Holland were once marine area, greatly influenced by the

surrounding seawater systems such as the Zuiderzee. Once a saline bay, it is nowadays a shallow freshwater lake in the north central Netherlands, known as the IJsselmeer. On the other hand, sites C and D are riverine area, developed under the influence of river systems such as Rhine and Meuse.

Paleoenvironmental background of the Holocene peat helps us understand the conditions under which the peat samples had developed. The Holocene peat can be subdivided into basal peat and intercalated peat. Basal peat overlays pre-Holocene surfaces, such as Pleistocene deposits, and its formation is associated with the phase of decreased drainage during the Holocene sea-level rise. During the phase of sea-level rise ($\sim 8 \text{ mm yr}^{-1}$), the groundwater table had risen so high that the land surface was waterlogged (Brew, Horton, Evans, Innes & Shennan, 2015). This is marked by the accumulation of basal peat, which was followed by intertidal mudflat layers, mainly consisting of clay and silt. Clay and silt thus mark the beginning of the marine influence. Salt marshes formed during the transition from clay and silty marine deposition to peat (3800 BP). This was followed by peat formation at approximately 3500 BP (Brew et al., 2015). This indicates the beginning of fresh water influence. Although the rate of sea level rise had become relatively stagnant (4000 BP), sea level continued to rise by 2 mm yr^{-1} . (Brew et al., 2015). The mixing of seawater and fresh water created a brackish environment, which contains a high amount of pyrite. On top of the mudflat layers and salt marsh depositions, intercalated peat formed. Its formation occurred under the influence of a relatively slow rate of sea-level rise and brackish water.

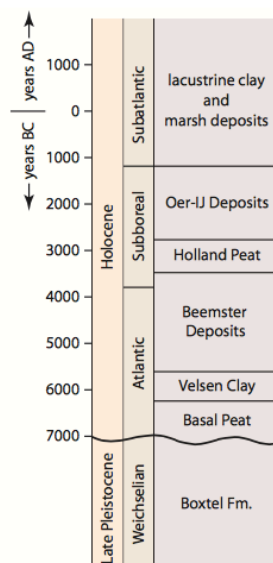


Figure 3. Holocene stratigraphy column. Taken from Donselaar and Geel (2007)

Methods

Table 1 below summarizes basic information on samples site A, B, C, and D, which include: the depth of samples collected and used for extraction; groundwater table depth; and the number of samples used from each location. Duplicate samples were taken from every third sample. 120 samples were used in total for the extraction of S.

Sampling

First, a core from each site was drilled to acquire a sediment description and to determine the depths to be sampled. The first 20 to 100 cm was drilled with an Edelman auger. A gouge auger (3 cm diameter) was used as soon as peat was found. The core was sliced into 10 cm pieces inside the gouge auger and subsequently each piece was transferred into a plastic bag. Each bag was labeled and placed in an airtight glass jar containing an Anaerocult C bag to keep the jar anaerobic. This procedure was done as quickly as possible to prevent oxidation of the samples as much as possible. The depth of groundwater table was measured in the borehole using a flat tape water level meter. The depth ranges to be sampled and analyzed were

determined on site, based on the visibility of peat substances. For example, partial segments of the sediment core in site D were sampled and analyzed to avoid sampling clay layers.

Table 1

Information about the sampling sites

| | Location | Depth range sampled (cm below surface) | Depth range used for analysis (cm below surface) | Groundwater table depth (cm below surface) | # Sample | # Total sample |
|--------------------|---|--|--|--|-----------------------|----------------|
| Site A | 52° 29' 16.3536" N 5° 2' 16.9656" E | 45 - 400 | 45 - 340 | 72 | 30 + 10 duplicates | |
| Site B | 52° 24' 0.738" N 4° 58' 43.2732" E | 20 - 200 | 20 - 200 | 50 | 18 + 6 duplicates | |
| Site C | 51° 56' 55.9644" N 4° 54' 40.2804" E | 100 - 300 | 100 - 300 | 91 | 20 + 6 duplicates | |
| Site D | 51° 50' 56.8896" N 4° 56' 32.3088" E | 100 – 210, 250 – 260, 380 – 500 | 100 – 210, 250 – 260, 380 – 490 | 85 | 23 + 7 duplicates | |
| All sites combined | | | | | | 120 |

Sequential wet chemical extraction of 1) AVS, 2) elemental sulfur, and 3) CRS

The extraction of acid volatile sulfur (AVS) was performed inside the glove box. All chemicals were purged with nitrogen gas before being placed inside the glove box. The quantification procedure of AVS and the rest of the experiment (step 2 and 3) were carried out in the fume hood. The centrifuge tubes were flushed with argon gas while adding solutions that were purged with nitrogen gas.

Step 1: Acid volatile sulfur (FeS). The first step is the sequential wet chemical extraction of acid volatile sulfur. During the extraction, the AVS is converted to H₂S by 6M HCl and trapped in an alkaline Zn acetate solution. The S content of the trap solution is subsequently

determined by iodometric titration.

The extraction of AVS was done using the Burton diffusion method (Burton et al., 2009). 2-2.5 grams of wet sample was weighed into a 50 mL centrifuge tube. The trap solution consists of 20% zinc acetate solution containing zinc acetate and milliQ in a 1:5 ratio. The alkaline Zn acetate solution must be freshly prepared by adding 100 mL ZnAc solution to 400 mL 2M NaOH solution while being stirred. Once the trap solution was prepared, 10 mL centrifuge tube with 7 mL of this alkaline ZnAc solution was placed in the 50 mL centrifuge tube. 2 mL of ascorbic acid solution and 10 mL of 6M HCl were added and shaken overnight at 150 rpm. The next day, ZnS trap solutions were taken out, and the 50 mL centrifuge tubes were centrifuged. The ZnS traps with caps were stored in a fridge prior to analysis.

The HCl supernatant yielded in the first step (AVS) was used to measure the sulfate content to check whether sulfur can be detected outside the ZnS trap. From the original HCl solution containing 10 mL of 6M HCl and 2 mL of ascorbic acid solution, 1mL of the solution was taken and diluted with 9 mL of milliQ. The S content in this solution was then analyzed by Inductively Coupled Plasma-Optical Emission Spectroscopy (ICP-OES).

The quantification of AVS was done via iodometric titration. The Zn trap suspension was transferred from 10 mL centrifuge tube into an Erlenmeyer, and the tube was rinsed five times with 10mL milliQ. 10 mL of 6 M HCl was added, and simultaneously, excess iodine solution was added so that a slight yellow or orange color persists. Although 5 mL of 0.025 M I₂ was the sufficient amount for a slight yellow color to persist in solution (in most of the samples), some required 20 or 30 mL of iodine solution for the color to persist. Subsequently, 1 mL of 0.05 M starch indicator was added to obtain a blue color as starch reacts with iodine. With a thiosulfate solution, the excess iodine is back-titrated until the solution turns clear. The concentration of

AVS in the sample can be calculated, as we know the volume and molarity of both the iodine solution and the thiosulfate solution, as well as the dry soil weight of the sample.

After the HCl supernatant was discarded, remaining sediment residue from was washed with 10 mL acetone to remove the remaining HCl and to allow for a more thorough mixing with toluene.

Step 2: Elemental sulfur (S^0). The second step is the extraction of elemental sulfur (S^0) using the toluene method. This is done as the elemental sulfur is dissolved in toluene and subsequently quantified with colorimetry (Barlett & Skoog, 1954). 25 mL of toluene was added. To suspend the sediment, the tube was first manually and vigorously shaken and subsequently shaken over two nights at 150 rpm and then centrifuged. Toluene was decanted, filtered, and stored for the colorimetric method.

The quantification of elemental sulfur was done via colorimetric analysis, during which the elemental sulfur was reacted with cyanide to form thiocyanide, forming a colored ferric thiocyanate complex in the presence of ferric chloride. Prior to analysis, the expected range of S^0 concentrations had to be determined from available data. Based on this, a calibration curve was prepared by adding 2000 μL sodium cyanide, 1000 μL methanol, and 2000 μL iron (III) chloride, to 200 ppm S stocks with different volumes (0, 10, 20, 40, 60, 100, 150, 200, 250, 300 μL). The solution was shaken and centrifuged at 3000 rpm for 5 minutes. After a total of 10 minutes, absorption of the solution was measured in a quartz cuvette at 465 nm. For samples, the same method was done with 1000 μL of toluene sample instead of the S stock.

After the toluene supernatant was discarded, remaining sediment residue from was washed with 10 mL acetone to remove the remaining toluene and to allow for a more thorough mixing with chromium.

Step 3: Chromium-reducible sulfur (FeS₂). The third step is the extraction of chromium-reducible sulfur (CRS). During the extraction, the pyrite-associated sulfur (S⁻) is reduced to S²⁻ and converted to H₂S in an acidic chromous chloride solution. Subsequently, the H₂S is trapped in an alkaline ZnAc solution and the S content of the trap solution is determined by iodometric titration. The extraction of CRS was done using the Burton diffusion method (Burton et al., 2009). The trap solution was prepared following the same procedure of step 1. The extraction procedure required preparation of a chromous chloride solution. First, 500 g of CrCl₃·6H₂O was dissolved in 32% HCl on a hot plate and diluted to 1 L with additional 32% HCl. 800 mL of this acidic Cr (III) solution was then transferred into a 1 L pyrex bottle containing 160 g of Zn grains (12 mm). This should be performed slowly and cautiously, as the resulting reaction is exothermic and effervescent. The acidic Cr solution was left to react with the Zn-shot for 2-3 hours, during which Cr(III) was reduced to Cr(II) shown by a solution color change from green to blue. This solution was prepared immediately prior to each batch of CRS extractions. Once this solution was ready, a 10 mL centrifuge tube with 7 mL of alkaline ZnAc solution was placed in the 50 mL centrifuge tube with sediment residue. Then, 10 mL of Cr(II)Cl₂ was added to the 50 mL tube and shaken for 4 days at 150 rpm. After 4 days, ZnS trap solutions were taken out, the 50 mL centrifuge tubes were centrifuged, and the CrCl₂ supernatant was removed. The ZnS traps with caps were stored in a fridge prior to analysis.

The quantification of CRS was done via iodometric titration, following the same procedure of step 1.

Step 4: CS analysis & total destruction. The remaining sediment samples were used to carry out other analyses, such as total destruction and CS analysis, after they were oven-dried. Three grams of wet samples were weighed into aluminum plates and oven-dried at 60°C for 48

hours. Then, they were ground to pass a 2 mm mesh screen and 0.2 g of the ground samples was transferred into ceramic vials. CS concentrations were measured using an elemental analyzer, Fison Instrument (model NA 1500 NCS). The water content of the samples was determined by weighing the sample before and after oven-drying.

Total destruction refers to the procedure of obtaining total element concentrations via digestion of the same material using a heated mixture of HF, HNO₃ and HClO₄. This mixture was then evaporated after which a gel-like residue remained. Subsequently, a second step with an H₂O₂ solution was used to oxidize all organic material. This was again evaporated. The residue was then dissolved in a 1M HNO₃ solution to be analyzed by ICP-OES (Spectro Arcos).

Results

The lithology of the sediment cores was analyzed. The depth ranges of lithology description mentioned below only cover the depth ranges sampled for this study. Core A comprised of only peat layers with almost no clay minerals (2-5%) in the whole section analyzed (45-350 cm). Alternating layers of peat and clay were present in Core C, of which the peat layers were relatively thicker than the clay layers. Interestingly, this is reflected in the depth profiles of S and Al, which will be discussed later. Core B comprised of a thick surficial peat layer (20-180 cm) overlying a silty clay layer (180-200 cm). The clay layer extends down to 300 cm depth, which is why it was not sampled. Alternatively, Core D composed of predominantly clay layers, except for a peat layer at 140-200 cm depth and a very thin layer present within the clay layer at 400-500 cm depth. The amount of organic matter was the highest in Core A, where its content averages to 75% over the whole section analyzed. Core C showed high organic matter content (85-90%) in the peat layers and low content (14%) in the clay layer. The organic matter in Core B and D displayed a similar pattern of high organic matter content in peat and low in clay layers.

Figure 5 displays the depth profiles for the solid, inorganic S species and total S. Despite the difficulty in making a direct comparison between the study sites due to the varying range of the depth of sediment cores, it is possible to observe that the total S content is almost identical at 100-200 cm depth across all four sites. At 100-110 cm depth, there is a peak in total S concentration of $1000 \mu\text{mol g}^{-1}$, which is followed by a decrease and then a rapid increase at 190-210 cm depth. These abrupt peaks in total S content coincide with the transition boundary between clay and peat layers. Other than these peaks, there are large variations in the total S content among four study areas. In Core A and the top section of Core D (100-220 cm), there is a general decrease of total S with depth. The rest does not show a significant pattern in total S.

Table 2 displays the averages of different inorganic S species, all values representing the fractions of total S in percentages. In all sites, pyritic S was the most abundant inorganic S form at all depths sampled. The next abundant species was AVS, followed by non-AVS in HCl. The levels of elemental S were strikingly low at all depths sampled. The AVS results for the 45-210 cm section of Core A were discarded, because of accidental mixing between the HCl solution and the ZnS trap solution during AVS extraction. On average, the sum of all three inorganic S species represents 33% of the total S pool in Core A, and 40% of that in Core B. The percentage was much higher for Core C and D, of which 86% and 72% of its total S were present as inorganic S, respectively.

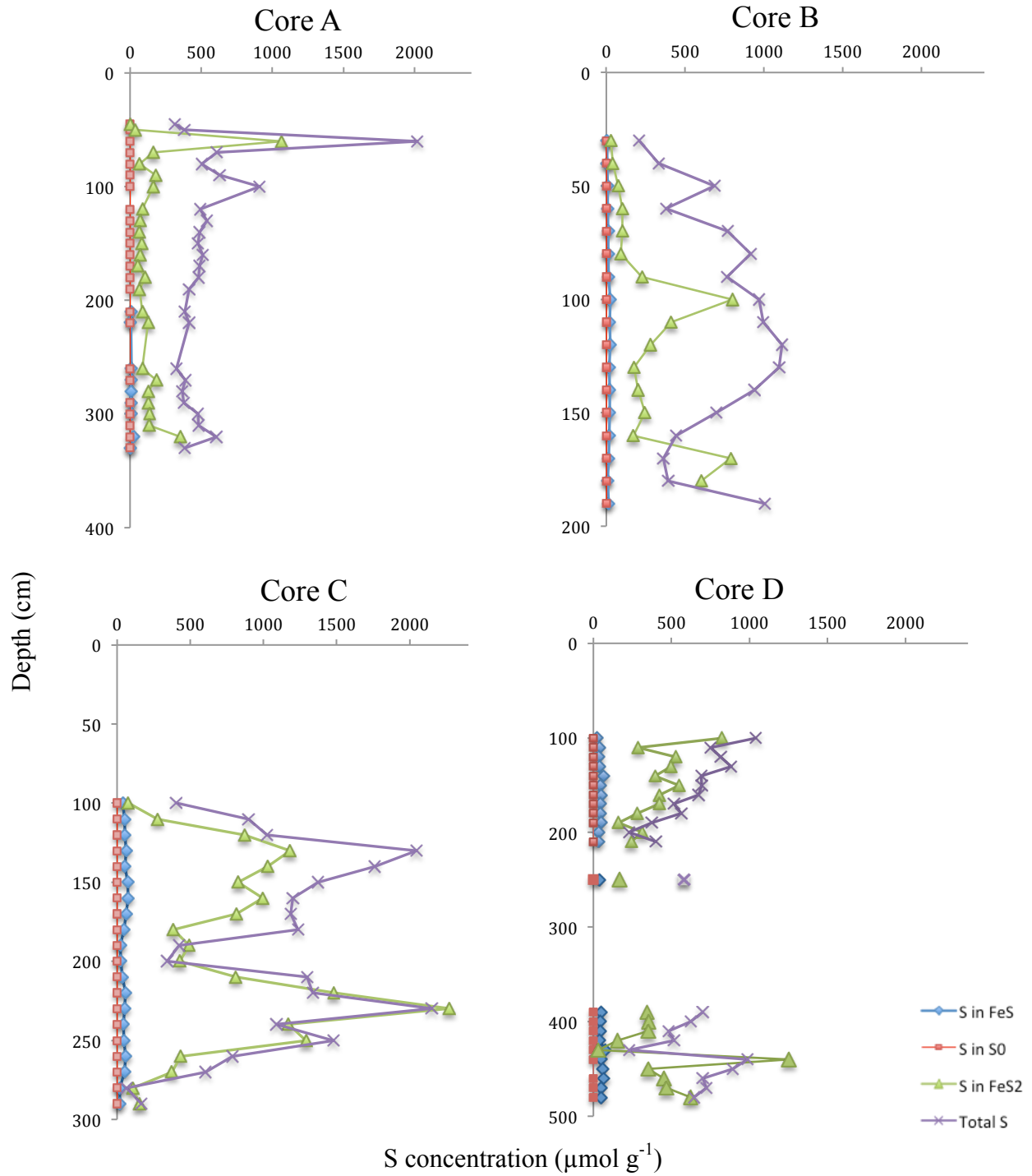


Figure 5. Changes in inorganic sulfur concentrations with depth in peat in four cores.

Table 2

Average fractions of inorganic S species as percentage of total S.

| | S in FeS | S ⁰ | S in FeS ₂ | S in HCl |
|--------|----------|----------------|-----------------------|----------|
| Site A | 2.02 | 0.08 | 25.35 | 1.10 |
| Site B | 2.22 | >0.01 (0.001) | 40.47 | 1.62 |
| Site C | 6.68 | >0.01 (0.0008) | 79.15 | 0.72 |
| Site D | 8.62 | >0.01 (0.0005) | 63.16 | 0.61 |

Likewise, it is possible to differentiate between the marine and the fluvial paleoenvironment based on their total inorganic S content. However, no clear distinction in the total S content could be made between samples from the marine and the fluvial paleoenvironment. The average concentrations of total S are: 422 $\mu\text{mol g}^{-1}$ in core A; 710 $\mu\text{mol g}^{-1}$ in core B; 1043 $\mu\text{mol g}^{-1}$ in core C; and 640 $\mu\text{mol g}^{-1}$ in core D. Core B demonstrated a higher total S content than core D, which makes it problematic to accept the hypothesis that the peat areas in the marine paleoenvironment has higher total S content than those in the fluvial paleoenvironment.

In order to estimate the approximate amount of organic S present in the study area, geochemical data of the nearby boreholes (partially published and partially unpublished by TNO) was used (Klein et al., 2015). The total organic carbon values were used to calculate organic S, based on the assumption that the C to S ratio is 110 to 1 (Stevenson & Cole, 1999). The calculated organic S fraction accounting for the total S pool in Core A and B were relatively high: 60% (288 $\mu\text{mol g}^{-1}$ average) and 50% (253 $\mu\text{mol g}^{-1}$ average) respectively. Organic S fractions in Core C and D were on the low side: 20% (159 $\mu\text{mol g}^{-1}$ average) and 30% (141 $\mu\text{mol g}^{-1}$ average) respectively. Since the vertical resolution of the data from the nearby boreholes is

much lower than that of the present study, the calculated percentages may lack accuracy and are thus rough estimates of organic S.

The findings show that the elemental sulfur contents are consistently low in all sites, accounting for less than 0.002% of total S. The amounts of elemental S present were trivial in comparison to other inorganic S species (Figure 5). There was no clear pattern of elemental S with depth. No significant negative correlation was found between elemental sulfur and reactive iron (Table 3).

Table 3

Correlation matrix showing Pearson's r for elemental sulfur and reactive iron. No significant correlation was found between the variables in all four cores, with $p > 0.05$.

| | Fe core A | Fe core B | Fe core C | Fe core D |
|-----------------------|-------------|--------------|--------------|-------------|
| S ⁰ core A | .133 (.546) | | | |
| S ⁰ core B | - | -.279 (.279) | | |
| S ⁰ core C | - | - | -.016 (.946) | |
| S ⁰ core D | - | - | - | .075 (.746) |

In general, pyritic sulfur concentrations form a parallel with the total sulfur concentrations in all sites except site B. This is indeed the case for Cores C and D, where pyrite is the dominant inorganic S species, accounting for 75 and 63 % of the total S pool respectively. The high pyrite content in Core C can be confirmed in Figure 6, which displays the scatter plot of S versus aqua regia extractable Fe. It illustrates a positive correlation between Fe and total S, indicating that almost all S is bound as pyrite S in all samples analyzed (100-300 cm). A weaker correlation between Fe and total S for samples from Core D shows that this relationship is less marked for this site. Averagely, the pyritic sulfur in Cores A and B contributes 25% and 40% to the total S pool, respectively. Site A shows low variability in pyrite content apart from a peak at

70 cm depth. Overall, substantially higher pyritic sulfur content is found at Cores C and D compared to Cores A and B.

Figure 7 shows depth profiles of total S, Fe and Al contents for all four sites. In general, Fe and Al appear to parallel each other in Cores A and B. Core A has a very low amount of clay in the whole section analyzed. This is reflected in the low Al content until a sudden peak at 330 cm depth. This peak coincides with the lithological transition from peat to clay. This is not the case in Cores C and D. In Core C, Al follows a vertical trend opposite to that of S and to a lesser extent that of Fe. The large fluctuation in S is due to the alternating presence of clay and peat layers. The relatively high Al content in Core D confirms the previous description of the lithology of Core D, which mostly consists of clay.

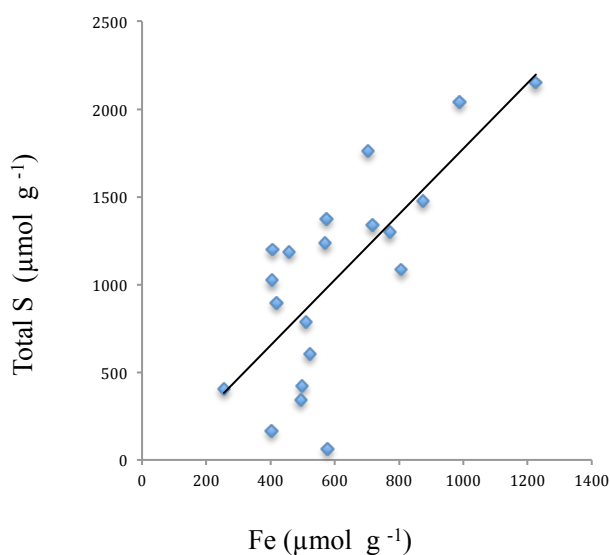


Figure 6 Relation between sulfur and iron contents in Core C as extracted by aqua regia. The trend line displays S:Fe relationship close to their stoichiometric relationship of 2:1.

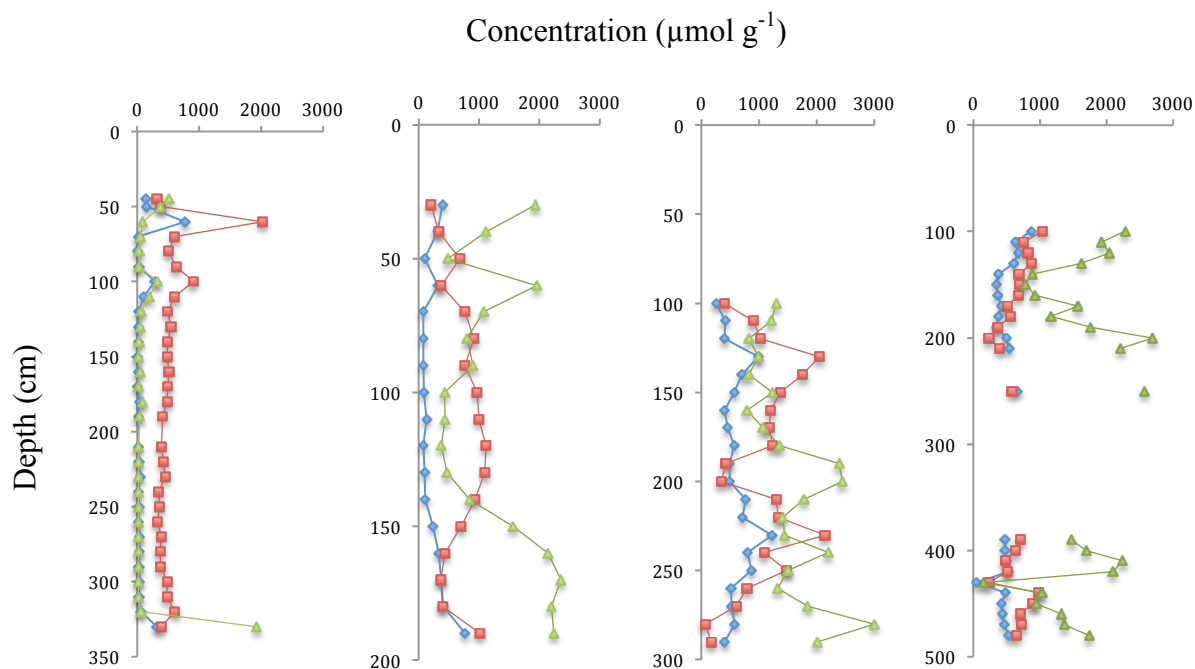


Figure 7. Depth profiles of total S (red), total Fe (blue), and Al (green), for cores A, B, C, and D (left to right).

Discussion

Researchers have found many different trends in the abundance of different inorganic S species in peat. Chapman (2001) and Wieder & Lange (1988) have revealed that pyrite is the most common form of inorganic S present in peat, whereas Casagrande et al. (1977) have reported different patterns of inorganic S forms in which the elemental sulfur was the dominant form of inorganic S. Altschuler et al. (1983) reported sulfate as the dominant inorganic S. Peat from Okefenokee Swamp (Florida, US) showed to have the trend of $S^0 > SO_4^{2-} > FeS_2 > H_2S$, where H_2S refers to aqueous H_2S (Casagrande et al., 1977). In Everglades peat (Florida, US), the general trend was $SO_4^{2-} > FeS_2 > FeS$ (Altschuler et al., 1983). Unlike the above studies that reported minor amounts of FeS_2 , two other studies found FeS_2 to be the dominant inorganic S species. In the Scottish peat bog, FeS_2 was the most abundant inorganic S species, showing a

general trend of $\text{FeS}_2 > \text{FeS} > \text{S}^0 > \text{SO}_4^{2-}$ (Chapman, 2001). A similar trend was found in peat from a Sphagnum-dominated area in West Virginia (Wieder & Lang, 1988). The findings of the present study are in line with those of Chapman and Wieder & Lang. Here, the order of abundance of inorganic S species is $\text{FeS}_2 > \text{FeS} > \text{SO}_4^{2-} > \text{S}^0$. It is important to note that the studies mentioned above have dealt with different types of peat, which most likely were formed under different environmental conditions. The environmental conditions, such as pH, availability of sulfate, sulfide and Fe, heavily influence the quantity and distribution of inorganic S species in peat.

To the best of my knowledge, this study is the first to document chemical analysis of elemental sulfur in Dutch peat. Overall, the elemental sulfur was a minor constituent in all four cores and no consistent spatial patterns were found. No positive or negative correlation between reactive iron and elemental sulfur was found, thus it is not possible to deduce any relationship between the presence of elemental sulfur in peat and the availability of reactive iron. Elemental sulfur is susceptible to oxidation and reduction, and it likely serves as an intermediate in processes that lead to pyrite formation by reacting with FeS, only if reactive iron is available (Urban et al., 1989). It can also react easily with organic constituents to form organic S (Casagrande et al., 1977). Such susceptibility of elemental sulfur makes it less probable that it accumulates. Given the high reactivity of elemental sulfur and the high pyrite contents in comparison to other studies, it seems that the majority of the elemental S that was originally present had transformed to become either pyritic S or organic S. This may explain the low concentrations of elemental sulfur found in this study.

In this study, it was hypothesized earlier that peat from a marine paleoenvironment would contain higher sulfur content than that from a fluvial paleoenvironment. Casagrande et al. (1977)

and Berner (1964) have concurred with this view, that marine peat contains higher sulfur content than non-marine peat. More specifically, the higher pyritic S content in marine peat was attributed to high organic matter content (Casagrande et al., 1977). They supported this by an additional finding that bacterial production of hydrogen sulfide occurs in marine peat but is limited in freshwater peat. Since the reaction between hydrogen sulfide and various iron compounds eventually leads to pyrite production, the abundance of hydrogen sulfide in peat is a key to variation in the pyrite concentration. Berner (1964) suggested that high pyrite content in marine peat is a result of sulfate diffusion, subsequently leading to hydrogen sulfide, which reacts with iron and elemental sulfur to form pyrite.

However, the findings from this study do not concur with this view. Rather, more inorganic S contents were present in the sediment cores from a fluvial paleoenvironment (sites C and D) than those in a marine paleoenvironment (sites A and B). Also, the pyrite fractions of total S (dominant inorganic S species) were much larger in the riverine areas. Although both riverine sites showed larger pyrite fractions of the total S pool than marine sites, the absolute S concentrations were on average higher in Core C ($774 \mu\text{mol g}^{-1}$) than in Core D ($412 \mu\text{mol g}^{-1}$). Based on the arguments above, it is tempting to conclude the same for the high pyrite content found in site C and attribute it to microbial activity yielding high levels of hydrogen sulfide. However, this explanation cannot hold for site C because it has been a non-marine environment. There must be other ways to interpret the high pyrite content in site C.

A more convincing explanation is that the high total S content observed at site C is due to the influence of brackish water as a result of paleoenvironmental evolution. Many have reported on the occurrence of high S contents in peat, which formed under the influence of brackish water (Casagrande et al., 1977; Lowe & Bustin, 1985; Lowe, 1986; Dellwig et al., 2001; Dellwig et al.,

2002). Dellwig et al. (2001) more specifically discussed the genesis of high pyrite contents, attributing it to the influence of brackish water and sea-level rise. During the phase of moderate sea-level rise in the Holocene epoch, the relatively low wave-energy conditions allowed mixing of freshwater and seawater. This resulted in brackish zones with variation in salinity, allowing for the enhanced degree of pyritization. They revealed that the maximum pyrite formation occurred under the influence of freshwater containing Fe-rich suspended matter and seawater that has a high SO_4 concentration, in the marshlands dominated by reed peat that had formed at relatively low average salinity. When applying this interpretation to the present study, the association of pyrite with brackish water environment explains the high degree of pyritization present in site C. The peat layers in fluvial paleoenvironment were overlain by peat formed under the influence of brackish or marine waters, which came to resemble brackish or marine peat in its S content and distribution (Price et al., 1991).

Despite the high pyrite contents and hence high inorganic S contents, there remains a fraction of unidentified S in the samples studied. There are several components that might explain this gap between the sum of the inorganic S fractions and the total S. First, the analysis of the remaining HCl solutions from the first step revealed presence of S. It is most likely that this S is sulfate from pore water or less likely gypsum, which probably formed in oxic peat during the condition of a low groundwater level. Nevertheless, the amounts of S measured in the HCl solutions were small, representing only 0.61-1.61% of the total S (Table 2). Second, it is possible that not all elemental sulfur present in peat was extracted during the extraction procedures. The colorimetric analysis of S^0 may have been unsuccessful due to the extremely low quantities of S^0 . When the sediment residues were being shaken for thorough mixing with toluene, it was visually noticed that some of the samples simply did not mix with it. This could

be due to incomplete washing of the sediment residue with acetone. However, the consistently low S^0 concentrations in the series of samples having variable total S contents suggests that such case is unlikely. Although some have acknowledged the presence of barite in peat, it is known that barite is highly insoluble and believed to be usually present in extremely small quantities.

Most of the unidentified fraction of total S is organic S. Others who have studied sulfur speciation in peat reported that most of the S is usually present as organic S rather than inorganic S. Casagrande et al. (1977) reported that sulfur in Okefenokee Swamp peat from a taxodium-dominated region was nearly 70% organic S, whereas a relatively lower percentage of 47% of sulfur as organic S in Florida Everglades. In Scottish peat bog, organic sulfur represented up to 64% of the total S pool (Chapman, 2001). In a sphagnum-dominated area in northern Minnesota, organic S is by far the most dominant constituent, accounting for 98% of total S pool (Urban et al., 1989). A study on peat from sphagnum-dominated area in Minnesota reported similar results, where organic S accounted for 78 to 89% of the total S pool (Wieder & Lange, 1986). Although the findings of the present study are not in line with the view that organic S is the dominant S form, it can be inferred from the abovementioned findings that the organic S accounts for a large part of the unidentified fraction of total S.

Understanding the mechanism of organic S formation may help interpreting the S content in both the marine and fluvial area. Organic S is often formed under the condition of a lack of available reactive iron. Reduction of sulfate yields hydrogen sulfide, and with a high sulfate reduction rate, excess hydrogen sulfide will be formed. This excess hydrogen sulfide may or may not form pyrite depending on the availability of reactive iron. When there is a lack of available reactive iron, hydrogen sulfide can no longer be converted to pyrite. Instead, it may react with humic substances to form organic S compounds. It is possible to apply this mechanism to

interpret the S depth profiles. Core C has the largest pyritic S fraction of 79% and the smallest organic S fraction of 20% out of total S. The high pyrite content and relatively low organic S forms found in site C suggests that the amount of reactive Fe available in peat was sufficient for the formation of high amounts of pyrite, making the formation of organic S secondary to that of pyrite. The lowest inorganic S content was found in Core A with distinctly low pyrite (Figure 5) and Fe content (Figure 7). The low availability of reactive Fe limits the formation of pyrite, seen by the paralleling depth profiles of pyritic S and Fe. Both profiles displays very low concentrations except for two peaks at 60 and 330 cm depth. With the competition of reduced sulfur species reacting with either organic matter or reactive Fe, the Fe-limiting condition favored the formation of organic S, resulting in organic S fraction accounting for averagely 60% of the total S.

There is variability in the stoichiometric ratio between organic S to organic C. The S to C ratio in peat may vary due to the uptake of S in organic matter during early diagenesis, which is influenced by the availability of iron in the sediment to a certain extent. It was assumed in all performed calculations that the stoichiometric relationship between organic S and organic C was 1:100. However, this ratio is a simple assumption based on the organic matter in mineral soils, which may not be necessarily relevant to peat (Stevenson & Cole, 1999). Tipping et al. (2016) measured S to C ratios in different types of peat and the ratios varied between 1:30 and 1:1000. In Price et al. (1991) the ratio fluctuates between 1:50 and 1:500, where the samples with pyrite were more between 1:45 and 1:107. The exact S:C ratio as well as the exact organic C contents of the samples obtained in this study is unknown. With such high variation in the S:C ratio in peat based on its type, and with the uncertainty in the presumed S:C ratio, the organic S and C contents could have been over or underestimated.

Conclusion

The findings in this study can be summarized into the followings: Pyritic sulfur was by far the most abundant form of inorganic S in all four cores, followed by acid-volatile S, sulfate, and elemental S; The amounts of elemental S were consistently low in all cores; and no significant correlation was found between elemental S and reactive Fe, and therefore it is difficult to establish a link between the presence of elemental S and the availability of reactive Fe. The findings also reveal a number of general features that distinguished riverine and marine peat. The riverine peat demonstrated higher S content than the marine peat, with inorganic S species accounting for a larger fraction of total S than organic S. On the other hand, the marine peat had more organic S than inorganic S. Nonetheless, the S content extracted in core C was exceptionally high in comparison to the other cores. This is attributed to the influence of brackish zone, where peat areas in site C probably developed with concurrent input of freshwater and seawater, leading to enhanced formation of pyrite.

References

- Altschuler, Z. S., Schnepfe, M. M., Silber, C. C. & Simon, F. O. (1983). Sulfur Diagenesis in Everglades Peat and Origin of Pyrite in Coal. *Science*, 221(4607), 221–227.
- Bartlett, J. K. & Skoog, D. A. (1954). Colorimetric Determination of Elemental Sulfur in Hydrocarbons. *Analytical Chemistry*, 26(6), 1008–1011.
<https://doi.org/10.1021/ac60090a014>
- Bates, A. L., Spiker, E. C. & Holmes, C. W. (1998). Speciation and isotopic composition of sedimentary sulfur in the Everglades, Florida, USA. *Chemical Geology*, 146(3), 155–170.
[https://doi.org/10.1016/S0009-2541\(98\)00008-4](https://doi.org/10.1016/S0009-2541(98)00008-4)
- Berner, R. A. (1964). Distribution and diagenesis of sulfur in some sediments from the Gulf of California. *Marine Geology*, 1(2), 117–140. [https://doi.org/10.1016/0025-3227\(64\)90011-8](https://doi.org/10.1016/0025-3227(64)90011-8)
- Brew, D. S., Horton, B. P., Evans, G., Innes, J. B. & Shennan, I. (2015). Holocene sea-level history and coastal evolution of the north-western Fenland, eastern England. *Proceedings of the Geologists' Association*, 126(1), 72–85.
<https://doi.org/10.1016/j.pgeola.2014.12.001>
- Brouns, K., Verhoeven, J. T. A. & Hefting, M. M. (2014). The effects of salinization on aerobic and anaerobic decomposition and mineralization in peat meadows: The roles of peat type and land use. *Journal of Environmental Management*, 143, 44–53.
<https://doi.org/10.1016/j.jenvman.2014.04.009>
- Burton, E. D., Bush, R. T., Sullivan, L. A., Hocking, R. K., Mitchell, D. R. G., Johnston, S. G., ... Jang, L. Y. (2009). Iron-Monosulfide Oxidation in Natural Sediments: Resolving Microbially Mediated S Transformations Using XANES, Electron Microscopy, and

- Selective Extractions. *Environmental Science & Technology*, 43(9), 3128–3134.
<https://doi.org/10.1021/es8036548>
- Casagrande, D. J., Siefert, K., Berschinski, C. & Sutton, N. (1977). Sulfur in peat-forming systems of the Okefenokee Swamp and Florida Everglades: origins of sulfur in coal. *Geochimica et Cosmochimica Acta*, 41(1), 161–167. [https://doi.org/10.1016/0016-7037\(77\)90196-X](https://doi.org/10.1016/0016-7037(77)90196-X)
- Chapman, S. J. (2001). Sulphur Forms in Open and Afforested Areas of Two Scottish Peatlands. *Water, Air, and Soil Pollution*, 128(1–2), 23–39.
<https://doi.org/10.1023/A:1010365924019>
- Dellwig, O., Böttcher, M. E., Lipinski, M. & Brumsack, H. J. (2002). Trace metals in Holocene coastal peats and their relation to pyrite formation (NW Germany). *Chemical Geology*, 182(2), 423–442. [https://doi.org/10.1016/S0009-2541\(01\)00335-7](https://doi.org/10.1016/S0009-2541(01)00335-7)
- Dellwig, O., Watermann, F., Brumsack, H. J., Gerdes, G. & Krumbein, W. E. (2001). Sulphur and iron geochemistry of Holocene coastal peats (NW Germany): a tool for palaeoenvironmental reconstruction. *Palaeogeography, Palaeoclimatology, Palaeoecology*, 167(3), 359–379. [https://doi.org/10.1016/S0031-0182\(00\)00247-9](https://doi.org/10.1016/S0031-0182(00)00247-9)
- Donselaar, M. E. & Geel, C. R. (2007). Facies architecture of heterolithic tidal deposits: the Holocene Holland Tidal Basin. *Netherlands Journal of Geosciences*, 86(4), 389–402.
<https://doi.org/10.1017/S001677460002360X>
- Erkens, G., van der Meulen, M. J. & Middelkoop, H. (2016). Double trouble: subsidence and CO₂ respiration due to 1,000 years of Dutch coastal peatlands cultivation. *Hydrogeology Journal*, 24, 551–568. <https://doi.org/10.1007/s10040-016-1380-4>

- Feijtel, T. C., Salingar, Y., Hordijk, C. A., Sweerts, J. P. R. A., Breemen, N. V. & Cappenberg, T. E. (1989). Sulfur cycling in a dutch moorland pool under elevated atmospheric S-deposition. *Water, Air, and Soil Pollution*, 44(3–4), 215–234.
<https://doi.org/10.1007/BF00279256>
- Hoogland, T., van den Akker, J. J. H. & Brus, D. J. (2012). Modeling the subsidence of peat soils in the Dutch coastal area. *Geoderma*, 171, 92–97.
<https://doi.org/10.1016/j.geoderma.2011.02.013>
- Klein, J., Van Gaans, P. & Griffioen., J. (2015). Geochemische karakterisering van de geotop van Holland (gebied 1b en 1c). TNO, 2015 R 10785, 419.
- Lamers, L. P. M., Tomassen, H. B. M. & Roelofs, J. G. M. (1998). Sulfate-Induced Eutrophication and Phytotoxicity in Freshwater Wetlands. *Environmental Science & Technology*, 32(2), 199–205. <https://doi.org/10.1021/es970362f>
- Lowe, L. E. (1986). Application of a Sequential Extraction Procedure to the Determination of the Distribution of Sulphur Forms in Selected Peat Materials. *Canadian Journal of Soil Science*, 66(2), 337–345. <https://doi.org/10.4141/cjss86-034>
- Lowe, L. E. & Bustin, R. M. (1985). Distribution of Sulphur Forms in Six Facies of Peats of the Fraser River Delta. *Canadian Journal of Soil Science*, 65(3), 531–541.
<https://doi.org/10.4141/cjss85-057>
- Marnette, E. C., Houweling, H., Dam, H. V. & Erisman, J. W. (1993). Effects of decreased atmospheric deposition on the sulfur budgets of two Dutch moorland pools. *Biogeochemistry*, 23(2), 119–144. <https://doi.org/10.1007/BF00000446>

- Nieuwenhuis, H. S. & Schokking, F. (1997). Land subsidence in drained peat areas of the Province of Friesland, The Netherlands. *Quarterly Journal of Engineering Geology and Hydrogeology*, 30(1), 37–48. <https://doi.org/10.1144/GSL.QJEGH.1997.030.P1.04>
- Postma, D. (1982). Pyrite and siderite formation in brackish and freshwater swamp sediments. *American Journal of Science*, 282(8), 1151–1183. <https://doi.org/10.2475/ajs.282.8.1151>
- Price, F. T. & Casagrande, D. J. (1991). Sulfur distribution and isotopic composition in peats from the Okefenokee Swamp, Georgia and the Everglades, Florida. *International Journal of Coal Geology*, 17(1), 1–20. [https://doi.org/10.1016/0166-5162\(91\)90002-Z](https://doi.org/10.1016/0166-5162(91)90002-Z)
- Roelofs, J. G. M. (1991). Inlet of alkaline river water into peaty lowlands: effects on water quality and *Stratiotes aloides* L. stands. *Aquatic Botany*, 39(3), 267–293. [https://doi.org/10.1016/0304-3770\(91\)90004-O](https://doi.org/10.1016/0304-3770(91)90004-O)
- Smolders, A. J. P., Lamers, L. P. M., Lucassen, E. C. H. E. T., Velde, G. V. D. & Roelofs, J. G. M. (2006). Internal eutrophication: How it works and what to do about it—a review. *Chemistry and Ecology*, 22(2), 93–111. <https://doi.org/10.1080/02757540600579730>
- Stevenson, F. J. & Cole, M. A. (1999). *Cycles of soils: Carbon, nitrogen, phosphorus, sulfur, micronutrients*. New York, USA: John Wiley & Sons.
- Tipping, E., Somerville, C. J. & Luster, J. (2016). The C:N:P:S stoichiometry of soil organic matter. *Biogeochemistry*, 130(1–2), 117–131. <https://doi.org/10.1007/s10533-016-0247-z>
- Urban, N. R., Eisenreich, S. J. & Grigal, D. F. (1989). Sulfur cycling in a forested Sphagnum bog in northern Minnesota. *Biogeochemistry*, 7(2), 81–109. <https://doi.org/10.1007/BF00004123>
- Vermaat, J. E., Harmsen, J., Hellmann, F. A., van der Geest, H. G., de Klein, J. J. M., Kosten, S., ... Ouboter, M. (2016). Annual sulfate budgets for Dutch lowland peat polders: The soil

- is a major sulfate source through peat and pyrite oxidation. *Journal of Hydrology*, 533, 515–522. <https://doi.org/10.1016/j.jhydrol.2015.12.038>
- Watanabe, Y., Yamaguchi, T., Katata, G. & Noguchi, I. (2013). Aerosol Deposition and Behavior on Leaves in Cool-temperate Deciduous Forests. Part 1: A Preliminary Study of the Effect of Fog Deposition on Behavior of Particles Deposited on the Leaf Surfaces by Microscopic Observation and Leaf-washing Technique. *Asian Journal of Atmospheric Environment*, 7(1), 1–7. <https://doi.org/10.5572/ajae.2013.7.1.001>
- Wieder, R. K. & Lang, G. E. (1986). Fe, Al, Mn, and S chemistry of Sphagnum peat in four peatlands with different metal and sulfur input. *Water, Air, and Soil Pollution*, 29(3), 309–320. <https://doi.org/10.1007/BF00158762>
- Wieder, R. K. & Lang, G. E. (1988). Cycling of inorganic and organic sulfur in peat from Big Run Bog, West Virginia. *Biogeochemistry*, 5(2), 221–242. <https://doi.org/10.1007/BF02180229>
- Wong, T. E., Batjes, D. A. J. & Jager, J. de (2007). *Geology of the Netherlands*: Royal Netherlands Academy of Arts and Sciences Amsterdam, Netherlands.
- Yu, Z., Beilman, D. W. & Jones, M. C. (2009). Sensitivity of northern peatland carbon dynamics to Holocene climate change. In A. J. Baird, L. R. Belyea, X. Comas, A. S. Reeve & L. D. Slater (Ed.), *Carbon cycling in northern peatlands* (pp. 55–69). American Geophysical Union. <https://doi.org/10.1029/2008GM000822>
- Zagwijn, W. H. (1986). *Nederland in het Holoceen*. Haarlem, the Netherlands: Rijks Geologische Dienst.